

Job No. 11126

STUDIES OF MANUAL CONTROL SYSTEMS  
Progress Report No. 5

for the Period 19 July 1964 to 18 October 1964

FACILITY FORM 902	N 65   1 6 8 1 0	
	(ACCESSION NUMBER)	(THRU)
	41	1
	(PAGES)	(CODE)
	CR-60697	05
	(NASA CR OR TMX OR AD NUMBER)	(CATEGORY)

1 December 1964

Submitted to:

National Aeronautics and Space Administration  
600 Independence Avenue  
Washington, D. C. 20546

Attention: Dr. T. L. K. Smull

GPO PRICE \$ \_\_\_\_\_

OTS PRICE(S) \$ \_\_\_\_\_

Hard copy (HC) \$ 2.00

Microfiche (MF) \$ 0.50

STUDIES OF MANUAL CONTROL SYSTEMS

PROGRESS REPORT NO. 5

for the Period 19 July to 18 October 1964

Contract NASw-668

1 December 1964

Submitted to:

National Aeronautics and Space Administration  
600 Independence Avenue  
Washington, D. C. 20546

Attention: Dr. T. L. K. Smull

TABLE OF CONTENTS

I.	INTRODUCTION . . . . .	1
II.	APPARATUS . . . . .	3
III.	THEORETICAL CONSIDERATIONS . .	5
IV.	RESULTS . . . . .	8
V.	EXPERIMENTAL PLANS . . . . .	20
VI.	REFERENCES . . . . .	21

## STUDIES OF MANUAL CONTROL SYSTEMS

### I. INTRODUCTION

This is a report of the work we have done under Contract NASw-668 during the three-month period beginning July 19, 1964 and ending October 18, 1964, the second quarter of the second year of the contract.

This report deals specifically with our investigation of multi-axis control systems and is a continuation of Part III of Progress Report No. 3, dated September 15, 1964.

This investigation has two aims: (1) to show the extent to which single-axis tracking behavior is indicative of multi-axis behavior, and (2) to show how coupling between the axes affects system behavior. We have attempted to quantify performance in terms of normalized mean squared errors and in terms of describing functions.

The preliminary experiments reviewed in Report No. 3 indicated that the performance in a given axis was degraded when the subject was required to track a second axis. Furthermore, two-axis performance worsened when the degree of coupling was increased. It was suggested in that report, however, that some of the degradation may have been due to a lack of training, rather than to an increase in the intrinsic difficulty of the task.

16810

16810

Four groups of experiments were conducted in order to investigate (1) the difference between single-axis and two-axis performance for input signals of various bandwidths, (2) the difference between single- and two-axis tracking for controlled elements of various complexities, (3) the effect on two-axis performance of input coupling, and (4) the effects of output coupling. A single, highly experienced tracker was used. The results of these experiments indicate that with sufficient training the tracker can control each axis of a two-axis situation as well in either axis in a single-axis task when the conditions on the two axes are the same. Furthermore, the effects of input coupling can be greatly reduced with practice.

*Author*

## II. APPARATUS

A compensatory tracking display, consisting of an error dot and a circle, was presented on the face of an oscilloscope 12 cm in diameter. The subject's task was to keep the dot as close to the center of the circle as possible. An 11" nylon stick attached to a force-sensitive hand control enabled the subject to influence the motion of the dot. The end of the stick deflected 1 cm per pound of applied force. The control-display relationship was 15 cm of error displacement per second<sup>2</sup> per centimeter of stick deflection when a second-order controlled element was used, 15 cm/sec/cm for a first-order system, and 1.5 cm/cm when the dynamics were proportional.

In order to provide a high degree of control-display compatibility, the control was oriented so that the stick was horizontal and could be moved in a plane parallel to the scope face. The response to a deflection of the stick was in the same direction as the stick motion when there was no cross coupling. A block diagram of the control situation is shown in Fig. 1.

The diameter of the circle was varied in order to present to the subject a continuous measure of his performance in terms of mean squared error. The relation of circle diameter to error was  $D(t) = K \overline{E^2(t)} + D_0$ , where  $D(t)$  was the diameter of the circle,  $D_0$  was 0.3 cm (the smallest allowable circle diameter),  $K$  a constant, and  $\overline{E^2(t)}$  the short-term mean squared error. To obtain  $\overline{E^2(t)}$ , the instantaneous squared error on

the X axis was added to that on the Y axis; the sum was passed through a low-pass filter having a time constant of ten seconds.

It was not clear at first how the circle diameter should be handled in order to provide the best experimental control. During the first phase of training the value of K was kept constant so that the relationship between circle diameter and mean squared error would be the same for all tasks. On the basis of experimental results (discussed in Section IV) we modified our procedure for controlling circle diameter. The constant K was adjusted at the beginning of each experimental run to provide a circle of 0.8 cm on the average for all tasks. Thus, the harder the task, the smaller the value of K. This arrangement provided an incentive to the subject that was independent of the difficulty of the task.

The input forcing function was pseudo-Gaussian and consisted of two signals having low-pass rectangular spectra. The cutoff frequency of the primary signal was 1.5, 2.5, or 4.0 rad/sec; the cutoff frequency of the secondary signal was 9 rad/sec in all cases, and the power level was 26 db below that of the primary signal. The composite signal was adjusted to produce a 1.25 cm rms movement of the dot in a given axis. The forcing function applied to the X axis was uncorrelated with that applied to the Y axis. Mean squared errors were computed separately for each axis over 2-1/2 minute intervals. These averages were taken over the same portion of the input during each run.

### III. THEORETICAL CONSIDERATIONS

#### A. INPUT COUPLING

A flow diagram of the two-axis compensatory tracking situation with input coupling is shown in Fig. 2. The type of coupling shown here is called input coupling because an input (i.e., stick deflection) to the controlled element along a given axis generally produces a vehicle (controlled element) response in both axes. The linearized human operator and the controlled element are each treated as a two-port network; the H's and C's represent the system describing functions relating the inputs and outputs of the respective networks.  $n_x$  and  $n_y$  are noise signals to account for the non-linear or time-varying behavior of the human operator. By definition,  $n_x$  and  $n_y$  are the components of the operator response that are linearly correlated with neither of the forcing functions ( $i_x$  and  $i_y$ ). All signals and system elements are functions of frequency; the argument ( $j\omega$ ) has been omitted for convenience. Because of the necessity to differentiate between signals on the two axes, we have adopted a notation different from that which has appeared in the literature pertinent to single-axis systems.

The particular type of input coupling investigated was a pure rotation of the control-display relationship. The optimal strategy for the human operator in this situation is to decouple the system by rotating his own input-output relationship by an equal and opposite amount; if he does so, he will be able to use the same basic describing function to



track as well as he does when there is no cross coupling. Except for the cross terms in the human operator's response, the decoupled system reduces analytically to the situation in which there is no coupling between the axes; that is, the human responds to an error in  $X$  in such a way that no error is introduced in  $y$ . The human describing functions may be found by ratios of input-stick and input-error transfer functions, or by direct measurement of error-stick relationships if the recirculating noise is small.

The describing functions are not so readily found when the operator fails to decouple the system. For example, the linear relationship between  $e_x$  and  $s_x$ , is not simply  $H_{xx}$ . Figure 2 shows that there is another linear path involving  $H_{xy}$ ,  $C_{yy}$ , and  $H_{yx}$ . Thus, neither the ratio of the x-axis input-stick and input-error describing functions nor a direct measurement of the linear relationship between  $e_x$  and  $s_x$  can be expected to yield the desired describing function  $H_{xx}$ .

One possible solution to this problem is the simultaneous determination of  $H_{xx}$  and  $H_{yx}$  through simultaneous measurement of the linear relationships between (1)  $e_x$  and  $s_x$ , and (2)  $e_y$  and  $s_x$ . That is, a model containing the two paths is adjusted to provide the best match according to some suitable criterion between model output and x-axis stick response.

## B. OUTPUT COUPLING

Output coupling occurs when the output (vehicle response) on one axis contributes to the output in the other. A flow diagram of the system is shown in Fig. 3. When the operator is able to decouple the system, analytical techniques applicable to single-axis systems may be applied to this situation. When the system is not fully decoupled, simultaneous measurements of two describing functions may be necessary as discussed in the preceding section. In contrast to the input-coupled situation, the complexity of the output-coupled situation may dictate that the optimum strategy for the human controller is not to attempt to decouple the system.

## IV. RESULTS

## A. SINGLE-AXIS VS. TWO-AXIS PERFORMANCE VS. BANDWIDTH

The experimental procedure was as follows: A pair of uncorrelated signals having identical spectra were selected to serve as the two forcing functions. Forcing functions of three cutoff frequencies ( $w_1$ ) were investigated: 1.5, 2.5, and 4.0 rad/sec. The controlled element dynamics were pure acceleration in both axes. The subject was required to track first in the X axis only, with the error dot constrained to move horizontally. He then tracked in the Y axis only, and finally in both axes simultaneously.

The normalized mean squared error (ratio of the mean squared error on a given axis to the mean squared input) was taken as a measure of the tracking performance. This performance is summarized in Table I, in which data obtained during single-axis tracking is compared with that obtained in the two-axis situation. There is no differentiation between x-axis and y-axis measurements.

If we consider measurements taken only after the subject was well trained in the particular task (as was done in compiling Table I), there are no significant differences between single- and two-axis tracking under any of the three conditions investigated in this set. Figure 4 shows, however, that during the early training session with an input bandwidth of 4 rad/sec there was a clear degradation of performance between the one- and two-axis situation. Initially, the error in a

given axis was approximately doubled by the additional requirement of tracking a second axis. As training progressed, the performance in both the single- and two-axis situations improved and the differences between the two decreased. The learning curves pertaining to input bandwidths of 2.5 and 1.5 rad/sec are presented in Figs. 5 and 6. Neither of these shows a consistent difference in single-axis and two-axis learning behavior.

Experiments with the lowest bandwidth were discontinued because the normalized errors were so low (less than 0.03) as to make the situation relatively uninteresting. A forcing function having a bandwidth of 0.96 was tried but was discontinued when the subject complained of fatigue and extreme difficulty in tracking the signal.

Figure 7 shows that normalized squared error increased almost linearly with bandwidth. Each datum point represents the average of the single-axis and two-axis performances shown for the corresponding frequency in Table I. We have not been able to find a simple explanation for this interesting relationship.

The describing functions corresponding to this set of experiments are shown in Figs. 8-a to 8-f. The left-hand column of Bode plots is for single-axis tracking, whereas the right-hand column is for the two-axis situation. Bode plots exhibited in the same row represent the responses to identical segments of the forcing function. The forcing-function bandwidths were, from top to bottom, 1.5, 2.5, and 4.0 rad/sec.

The measurements were made directly from error to operator output, rather than computed as  $\phi_{is}/\phi_{ie}$ . Because of the relatively good linear match--generally better than 80%--and the reasonableness of the results, we concluded that recirculating noise due to the operator's remnant did not significantly affect our measurements.

When the bandwidth was 1.5 rad/sec, the amplitude ratio for the two-axis situation was higher than in the single-axis situation by 2-6 db in the range of 1 to 8 rad/sec. The difference between single- and two-axis conditions was most noticeable when the bandwidth was 2.5 rad/sec. The single-axis plot (Fig. 8-c) showed a lead extending from below 0.25 rad/sec up to 2 rad/sec. On the other hand, the gain during two-axis tracking was flat up to 1 rad/sec and contained a lead beginning at that frequency.

Figures 8-e and 8-j show that the human describing functions corresponding to single- and two-axis conditions were very similar when  $w_1$  was 4.0 rad/sec. Dissimilarities between these two diagrams were much less than dissimilarities among Bode plots obtained under supposedly identical experimental situations. Figure 9 shows transfer functions obtained from three consecutive segments of data under the single-axis condition ( $C = K/s^2$ ,  $w_1 = 4.0$  rad/sec). The curves in the right-hand column represent data gathered a month after that pertaining to the left-hand set of curves. The differences between the top row of curves and the bottom row reflect either a time variation in the operator's behavior or an anomaly in the measurements arising from the nature of the time signals.

We lean towards the latter view because of the shape of the gain curves displayed in the bottom row, both of which contain a peculiar dip near  $1/2$  rad/sec. Note that the Bode plots in the right-hand column show a slightly greater over-all gain than the corresponding plots in the left-hand column. This result is in keeping with the improved performance that occurred because of the additional training received during the intervening period.

The results shown in Figs. 8-a through 8-d suggest that the operator tracked with a smaller x-axis error in the two-axis situation than in the single-axis situation for the period of time represented by the curves. (Unfortunately, we did not record the mean squared errors during this set of runs.) It is possible that the operator was not fully loaded in either the single- or two-axis situation and thus was able to improve his performance through greater effort in the latter case. Furthermore, since at the time of the measurements the relation between circle diameter and MSE was the same for all experiments, the operator would have had roughly twice the incentive in the two-axis situation.

In summary, we conclude that during these experiments the subject was limited by the bandwidth of his visual-motor response but not by his ability to process information. This conclusion is based on the following findings: (1) increase in the bandwidth of the forcing function produced an increase in normalized error, and (2) the addition of the second axis of tracking, which doubled the required information processing rate but did not affect the motor bandwidth requirements, did not produce consistent increases in error.

## B. SINGLE-AXIS VS. TWO-AXIS PERFORMANCE VS. DYNAMICS

Table II compares single- and two-axis performances obtained with the three kinds of dynamics investigated. (The dynamics were the same in both axes in the two-axis task.) The bandwidth of the input signal was 2.5 rad/sec in all instances. No statistical analysis of the data relating to K and K/s dynamics can be given, since the subject was not extensively trained under these conditions. As expected, the normalized mean squared error increased as the order of the controlled element increased. On the other hand, there appeared to be no consistent differences between single-axis and two-axis performance.

Bode plots for the three types of dynamics investigated are shown in Fig. 10. The input bandwidth was 2.5 rad/sec for all measurements. Figures 8-c and 8-d have been repeated as Figs. 10-e and 10-f for comparison with the results obtained with K and K/s dynamics. The amplitude ratio curve of Fig. 10-b, for two-axis tracking with K dynamics, differs from the amplitude ratio curve of Fig. 10-a in that it is about 2 db higher at all frequencies. The phase curves do not differ noticeably. Figures 10-c and 10-d for K/s dynamics show the same type of differences as seen with  $K/s^2$  dynamics. The low-frequency portion of the single-axis result shows a lead term, whereas the corresponding segment of the curve pertaining to two-axis tracking is flat, indicating tighter control in the two-axis situation. The enhanced two-axis performance could have been due to the increased incentive, as mentioned in the preceding section. It may also have been a result of the order in which these particular measurements were taken.

A comparison of the data obtained with the three kinds of dynamics reveal the same trends as shown by McRuer et al.<sup>1</sup> Figure 11 shows that the subject tended to maintain the same type of total open-loop behavior near crossover independently of the controlled-element dynamics. The gain decrement was roughly 6 db/octave, and the phase margins for  $K/s$  and  $K/s^2$  dynamics were about  $20^\circ$ . (We attribute the zero-phase margin indicated for  $K$  dynamics to a measurement error.) The crossover frequency was between 7 and 8 rad/sec with  $K$  and  $K/s$  dynamics and receded to 5 rad/sec with  $K/s^2$  dynamics.

The experiments described so far have involved only compatible-coordinate situations; that is, in all two-axis tasks the experimental conditions on the two axes have been as nearly identical as we could make them. In order to investigate the non-compatible-coordinate situation, the subject was given practice with different dynamics on each axis.  $C_{xx}$  was kept at  $K/s^2$ , whereas  $C_{yy}$  was either  $K$  or  $K/s$ . The bandwidth of the forcing function was 2.5 rad/sec. Figure 12 contains the learning curves for  $C_{yy} = K/s$ ; Fig. 13 pertains to  $C_{yy} = K$ . Plotted for comparison with these curves are the errors (taken from Table II) that were obtained with identical dynamics on both axes. Bode plots have not yet been obtained from this set of data.

Because the subject had not reached asymptotic performance when training was halted, the full capabilities of the tracker in the mixed-dynamics situation may not be indicated by the results of this set of experiments. We do see, at any rate, that there was a noticeable amount of interference between the two axes early in learning. That is, the performance on a



given axis was generally worse when the dynamics on the two axes were different than when they were identical. This type of behavior has been reported in the literature by Chernikoff and LeMay.<sup>2</sup>

To illustrate the interference occurring with proportional control on the Y axis and acceleration control on the X axis, let us compare errors obtained under the following three situations: (1)  $C_{xx} = C_{yy} = K$ ; (2)  $C_{xx} = C_{yy} = K/s^2$ ; (3)  $C_{xx} = K/s^2$ ,  $C_{yy} = K$ . Table II shows that errors obtained with proportional control on both axes (condition 1) were only one third of those obtained with acceleration control on both axes (condition 2). Thus, the system was easier to control when the controlled element dynamics were proportional rather than second order. On the other hand, when one axis was constrained to have second-order dynamics, it was easier to control the other axis when it had acceleration dynamics than when it had proportional control. That is, y-axis errors were greater under condition 3 than under condition 2, which result is in the opposite direction to that obtained by comparing the errors obtained under conditions 1 and 2.

The greatest amount of interference was seen in the situation just described ( $C_{xx} = K/s^2$ ,  $C_{yy} = K$ ). The greater effect was seen on the Y axis, in which the error (after training) was over three times that obtained with K dynamics on both axes. This observation is in keeping with the subject's comment that the Y axis was particularly difficult to control because the rapid control motions used in controlling the X axis produced unwanted motions in the Y axis. The x-axis error

was only 20% higher than when both axes had acceleration dynamics. The interference appearing in both axes when the dynamics were  $C_{xx} = K/s^2$  and  $C_{yy} = K/s$  was less than in the above case and was diminishing as training progressed.

We can explain the results of this experiment in the following way. First of all, the subject had a difficult learning task when  $C_{xx} = K/s^2$  and  $C_{yy} = K$ . If, as we assume, the subject tries to maintain the same over-all open-loop transfer function under all conditions, his own transfer function on the Y axis must differ from that on the X axis by two integrations. Secondly, he has a mechanical problem in keeping his intended x-axis control motions strictly along the horizontal axis. On this basis, we might expect less interference when  $C_{xx} = K/s^2$  and  $C_{yy} = K/s$ , since the required transfer functions and control motions in the two axes are less dissimilar than in the previous situation.

To summarize the results of the two sets of experiments so far reviewed, the two-axis tracking task may be considered as two independent single-axis tasks when the conditions on the two axes are the same. That is, when the subject is well trained, the normalized mean square error on a given axis is unaffected by whether or not the subject is simultaneously tracking a second axis. When the conditions on the two axes are different, however, the total squared error may not merely be the sum of the errors that would be obtained on each axis tracked individually. Early in learning, the error on a given axis increases when the subject is required to track a second axis having different control dynamics. The interference between

Job No. 11126

Bolt Beranek and Newman Inc

axes under these conditions can no doubt be reduced through extensive training. But because of the inherent complexity of the situation, it is not clear whether or not the interference can be eliminated.

## C. INPUT COUPLING

The axes were coupled in such a way that there was an effective rotation between the control and the display; the vector acceleration of the dot was at a predetermined angle with respect to the vector stick deflection. The sensitivity of the stick was in all cases  $15 \text{ cm/sec}^2/\text{cm}$ , as in the previously-described situations when no coupling was employed.

Rotations of 45, 60, and 90 degrees were used. Acceleration dynamics were used throughout this set of experiments; the bandwidth of the input signal was 1.5 rad/sec. The record of performance shown in Fig. 14 indicates that with training the subject was able to control a system having 45 to 60 degrees of rotation almost as well as one with no coupling. The variability of the data precludes generalizations about the trend of the performance when the rotation is  $90^\circ$ . The subject's performance in this particular task was highly dependent upon his alertness and state of well-being at the time of the experiment.

We have shown theoretically that if the subject is able to decouple the system, he can use the same basic describing function to track as well as he does when there is no cross coupling. Thus, the ability of the subject to track as well when there is 45 or 60 degrees of coupling as when there is no coupling suggests that he is able to decouple the system. These results are not proof of decoupling, however, since it is possible that the subject worked harder in the coupled situation to compensate for his inability to decouple the system. Supporting evidence ought to be obtained from

Job No. 11126

Bolt Beranek and Newman Inc

appropriate describing functions before final conclusions are made. (We expect to include such describing functions in our next report.)

## D. OUTPUT COUPLING

The system was coupled by processing the output of each controlled element and adding it to the output of the controlled element on the other axes as shown in Fig. 3. Thus, each controlled element contributed to the response of the system in both axes. Since the controlled elements and coupling networks were all second order, the relation between control movement in the other was fourth order. The transfer function of the controlled element was, as before,  $15 \text{ cm/sec}^2/\text{cm}$  of stick deflection. The coupling was 1, 2, 4, and 8  $\text{cm/sec}^2/\text{cm}$ . In the absence of an input forcing function, this calibration specifies the acceleration of the dot in one axes caused by vehicle displacement in the other.

The performance of the subject in this situation is shown in Fig. 15. The appropriate entry in Table I was plotted as a dashed line to illustrate his performance in the absence of coupling. Although the subject was able to control the output-coupled system as well as the uncoupled one when the coupling was  $1/\text{s}^2$  and  $2/\text{s}^2$ , the errors rose significantly as the amount of coupling was increased. The error increased by more than tenfold when the coupling was  $8/\text{s}^2$ . The experimental results obtained with this amount of coupling agree with our theoretical conclusions that the output-coupled system is basically more difficult to track than the uncoupled system. More training would be necessary before the relative difficulty of the  $4/\text{s}^2$  coupling could be determined.

## V.        EXPERIMENTAL PLANS

We have presented in this report the results of a set of preliminary experiments conducted on a single subject. We think some interesting trends have been indicated and are worth exploring with reasonable thoroughness. Consequently, a series of well-controlled experiments, employing at least four subjects, has been initiated. The primary object of this effort will be to determine to what extent models of the single-axis tracker apply to the two-axis situation when (1) conditions on the two axes are identical, and (2) conditions on the two axes differ.

REFERENCES

1. McRuer, D. T., et al., "Human Pilot Dynamics in Compensatory Systems: Theory, Models, and Experiments with Controlled Element and Forcing Function Variations," (forthcoming RTD-TDR).
2. Chernikoff, R. and LeMay, M., "Effect of Various Display-Control Configurations on Tracking with Identical and Different Coordinate Dynamics," *Journal of Experimental Psychology* 66, 95, 1963.



TABLE I  
Normalized Mean Squared Errors  
Acceleration Dynamics on Both Axes

Bandwidth, rad/sec	<u>1.5</u>		<u>2.5</u>		<u>4.0</u>	
	<u>1-Axis</u>	<u>2-Axis</u>	<u>1-Axis</u>	<u>2-Axis</u>	<u>1-Axis</u>	<u>2-Axis</u>
Tracking Situation						
Sample Mean	0.027	0.029	0.095	0.100	1.175	0.188
Estimated Standard Deviation of the Mean	0.005	0.006	0.005	0.004	0.008	0.017
No. of Datum Points	6	6	4	9	4	4
Period of Data Acquisition	7/29 - 7/31		9/14 - 9/18		9/14 - 9/18	

TABLE II

Normalized Mean Squared Errors  
Changes with Dynamics $w_1 = 2.5$  rad/sec;  $C_{xx} = C_{yy}$ ; no coupling

<u>Dynamics</u>	<u>Tracking Situation</u>	<u>Normalized Error</u>
K	single axis	0.034
K	two axes	0.034
K/s	single axis	0.056
K/s	two axes	0.054
$K/s^2$	single axis	0.095
$K/s^2$	two axes	0.100

Each entry relating to K and K/s dynamics is the average of two datum points (one x-axis and one y-axis measurement) obtained on 8/6/64. The entires for  $K/s^2$  are taken from Table I.

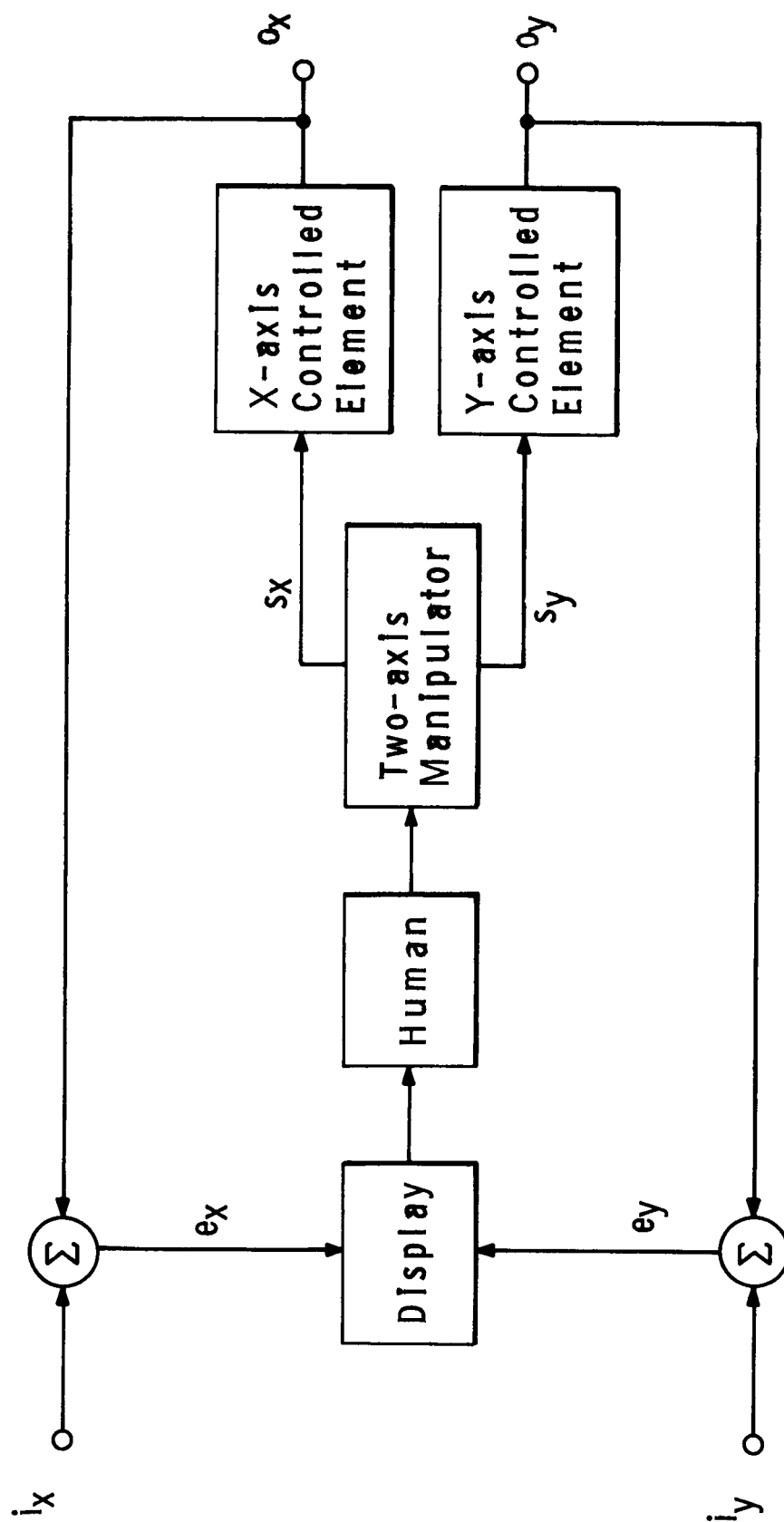


FIG. 1 COMPENSATORY TRACKING  
Two-axis Uncoupled System

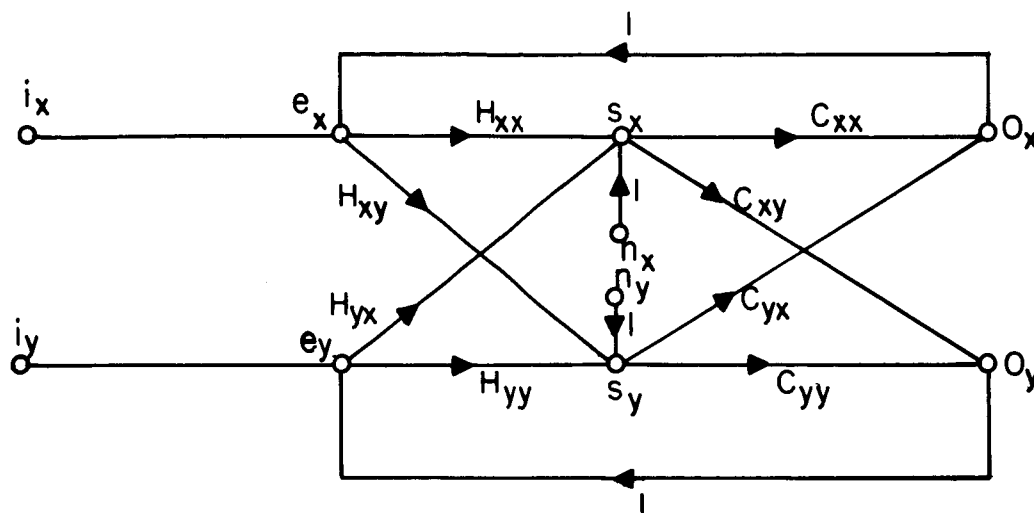


Figure 2. Two-Axis Compensatory Tracking with Input Coupling

- $i_x$  = x-component of the input forcing function.  
 $e_x$  = x-component of the error displayed to the human operator.  
 $s_x$  = x-component of the stick deflection (operator's response).  
 $o_x$  = x-component of the system output.  
 $n_x$  = x-component of the operator's response that is not linearly correlated with either  $i_x$  or  $i_y$ .  
 $H_{xx}$  = linear relation between x-component of operator's response and x-component of error.  
 $H_{xy}$  = linear relation between y-component of operator's response and x-component of error.  
 $C_{xx}$  = controlled element relating x-component of system output to x-component of stick deflection.  
 $C_{xy}$  = controlled element relating y-component of system output to x-component of stick deflection.

Signals and system functions in the Y axis correspond to those defined above for the X axis.

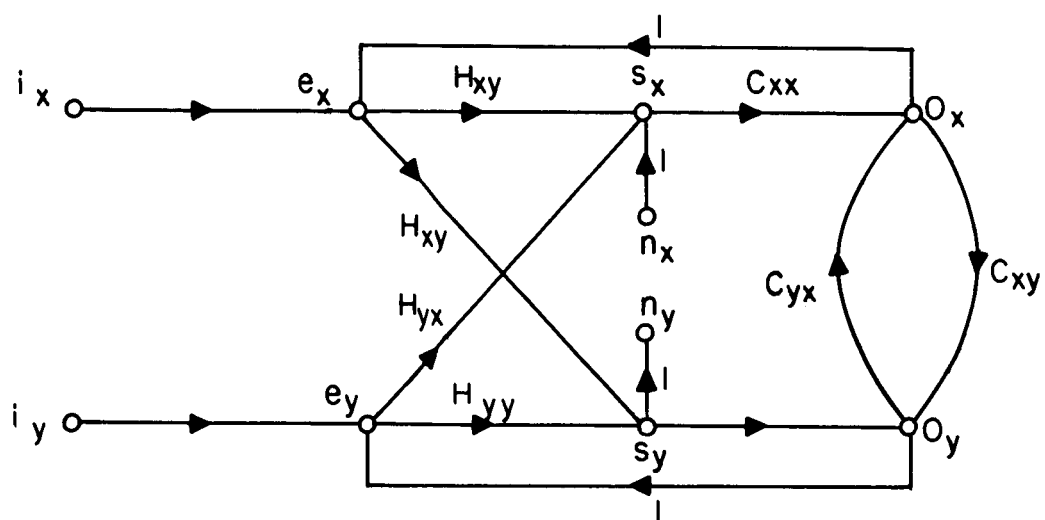


FIG.3 OUTPUT COUPLING

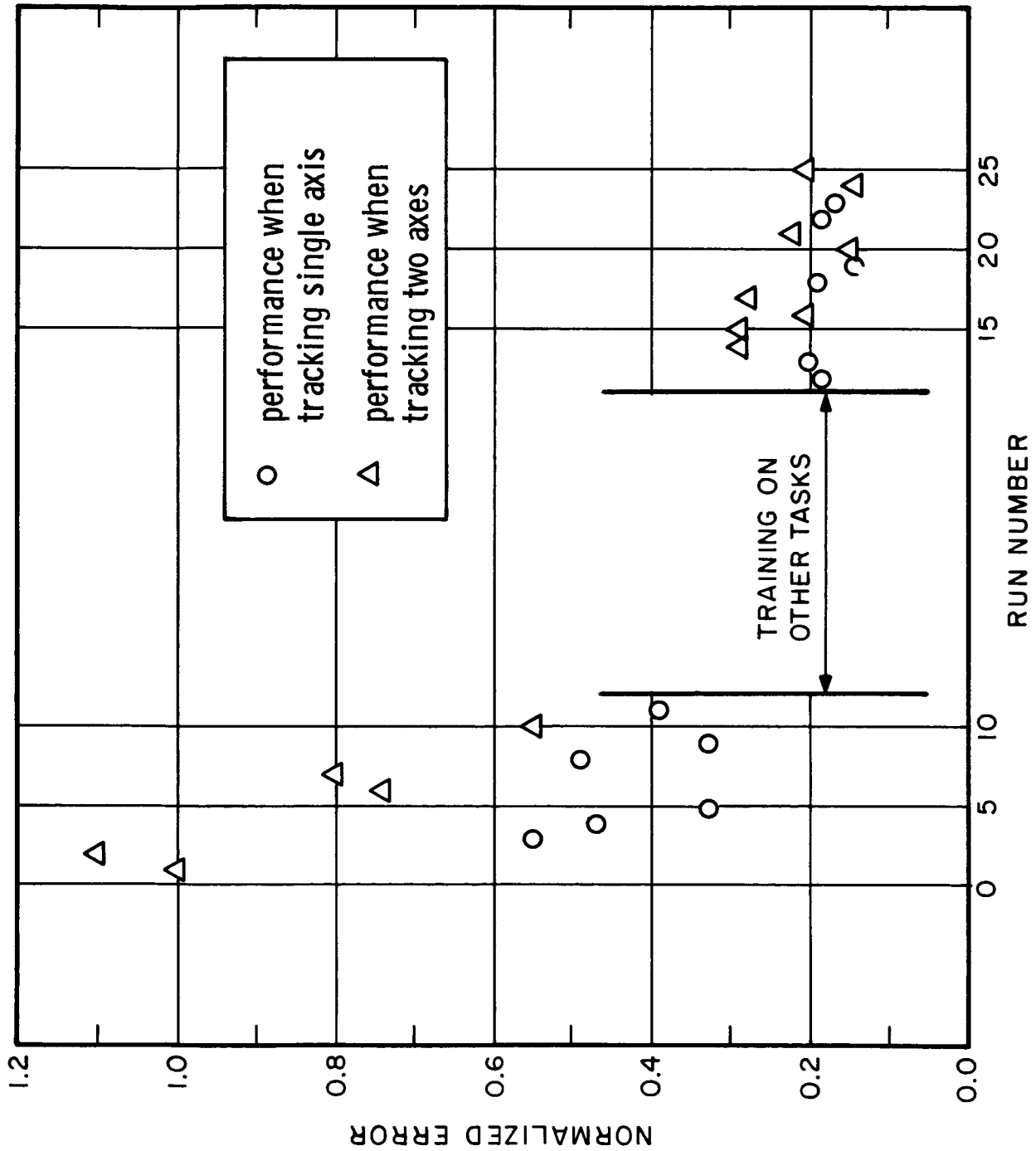


FIG. 4 SINGLE-AXIS AND TWO-AXIS PERFORMANCE  
 $C_{xx} = C_{yy} = K/s^2$   $w_i = 4 \text{ RAD/SEC}$

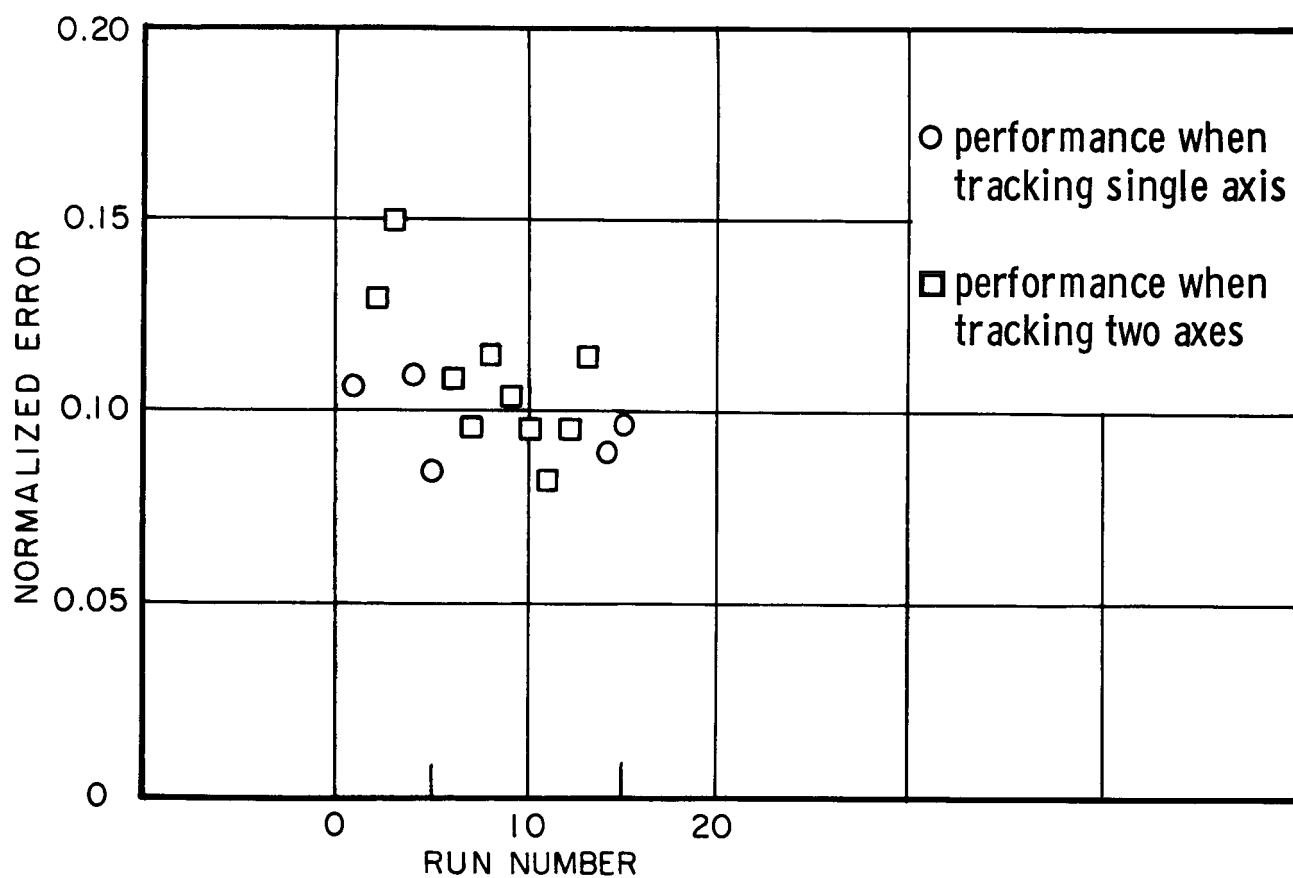


FIG. 5 SINGLE-AXIS AND TWO-AXIS PERFORMANCE  
 $C_{xx} = C_{yy} = K/s^2$   $w_i = 2.5 \text{ RAD/SEC}$

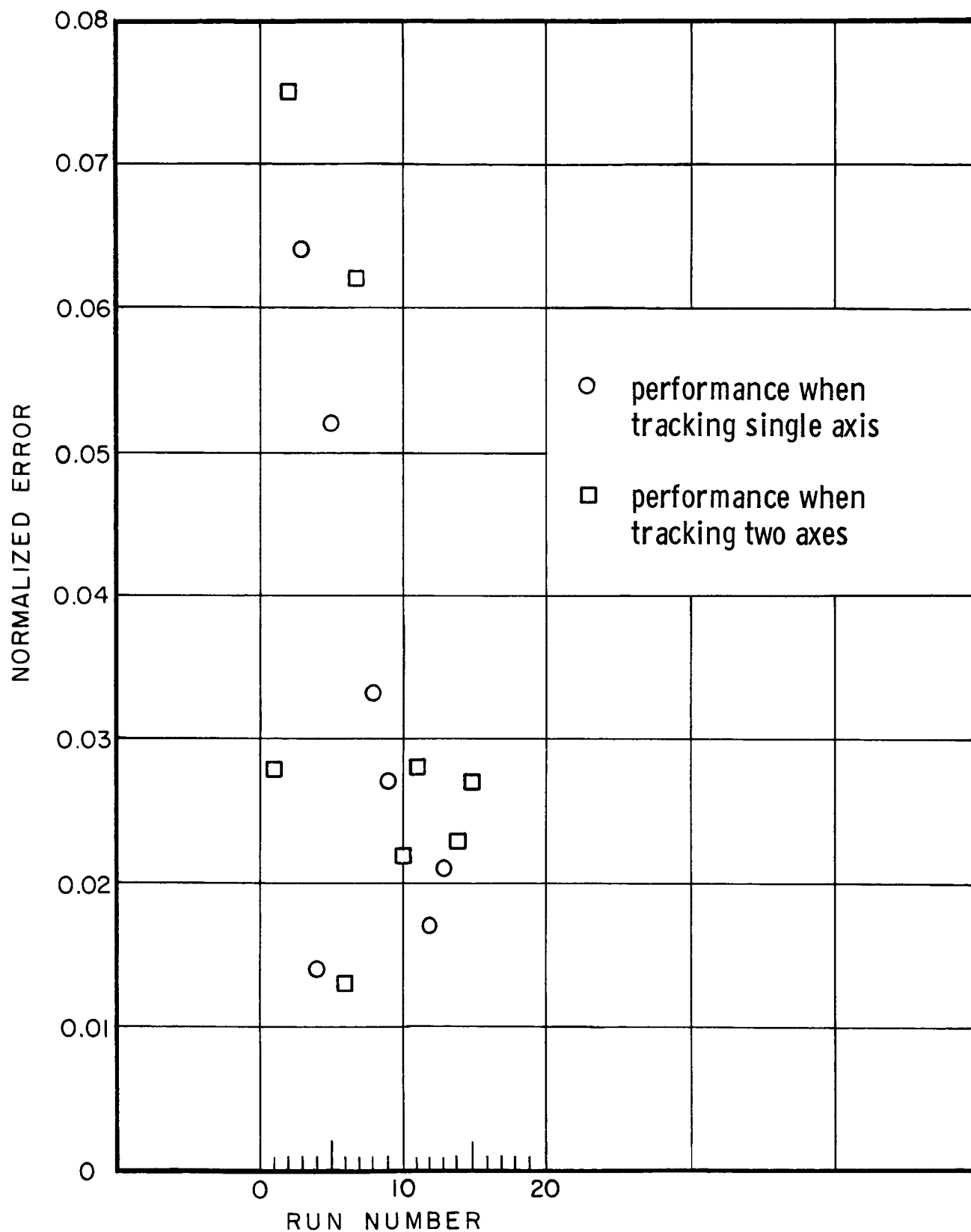


FIG. 6 SINGLE-AXIS AND TWO-AXIS PERFORMANCE  
 $C_{xx} = C_{yy} = K/s^2$      $w_i = 1.5 \text{ RAD/SEC}$



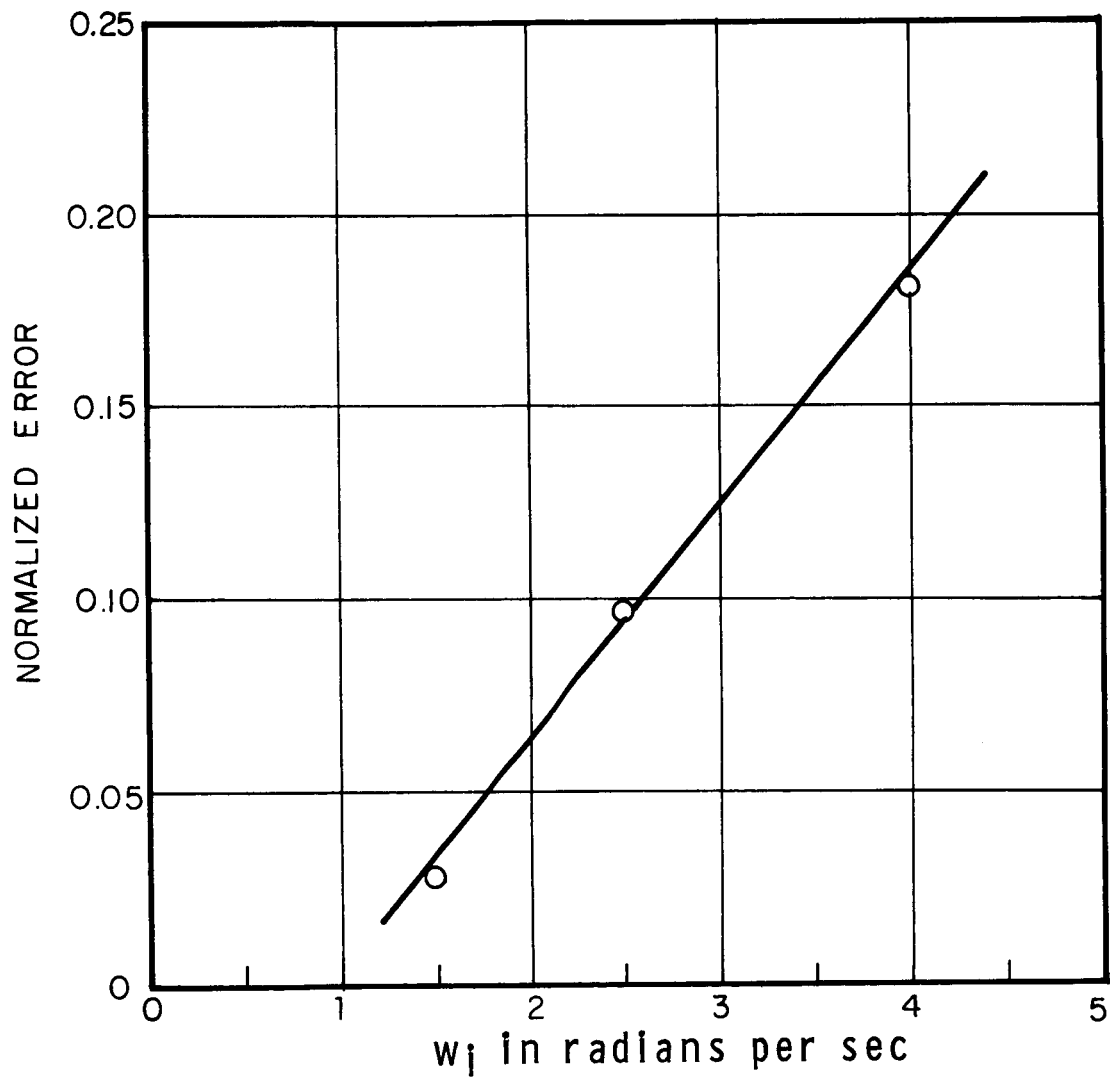
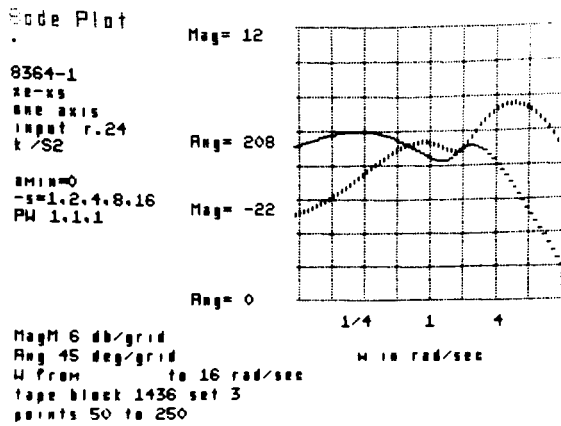


FIG. 7 ERROR vs BANDWIDTH

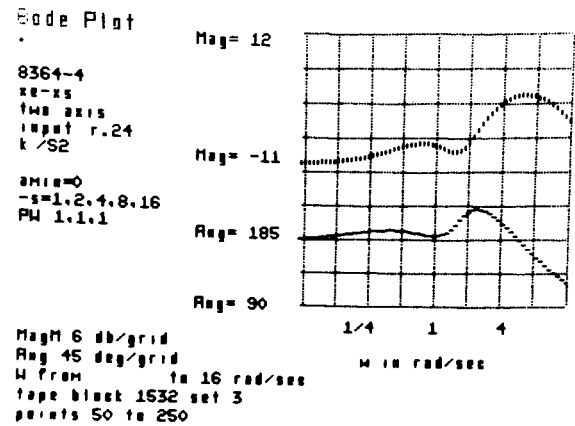
# FIG. 8 HUMAN OPERATOR DESCRIBING FUNCTIONS. CHANGES WITH BANDWIDTH

## Single-axis Tracking

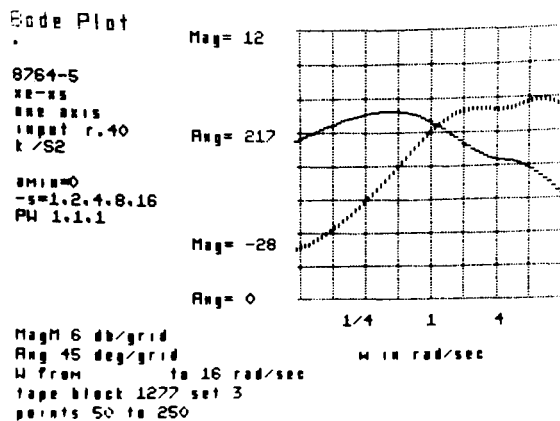


a

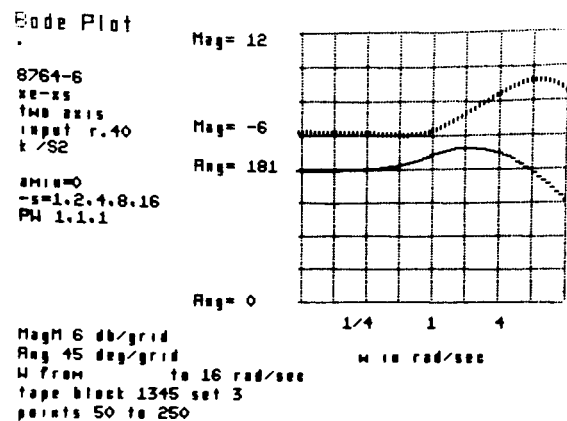
## Two-axis Tracking



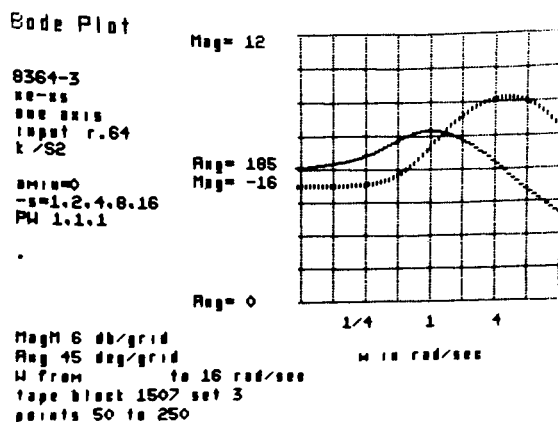
b

 $w_i = 1.5 \text{ rad/sec}$ 

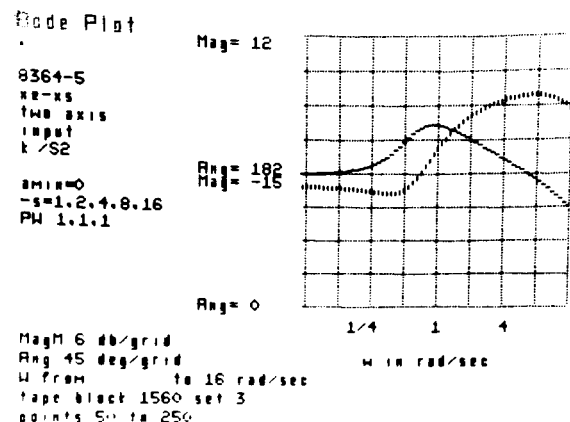
c



d

 $w_i = 2.5 \text{ rad/sec}$ 

e



f

 $w_i = 4.0 \text{ rad/sec}$

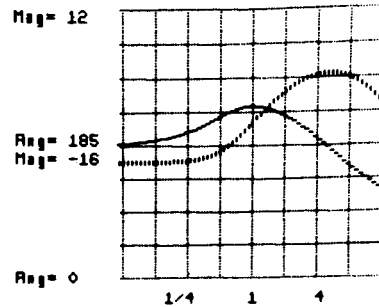
# FIG. 9 HUMAN OPERATOR DESCRIBING FUNCTIONS SUCCESSIVE RUNS UNDER IDENTICAL CONDITIONS

Single-axis.  $C = K/s^2$ 

Data taken 8/3/64

Bode Plot

8364-3  
 XE-XS  
 ONE AXIS  
 INPUT r.64  
 K/S2  
 SMIN=0  
 -S=1.2,4,8,16  
 PW 1.1,1



Mag 6 db/grid  
 Ang 45 deg/grid  
 W from to 16 rad/sec  
 tape block 1507 set 3  
 points 50 to 250

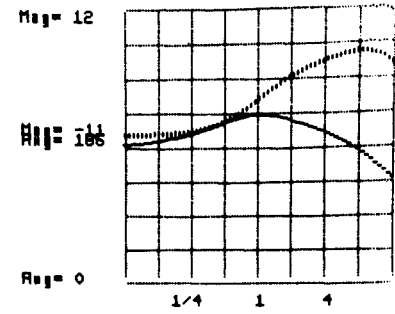
a

Input BW=4.0 rad/sec

Data taken 9/18/64

Bode Plot

91864-8a  
 XE-XS  
 ONE AXIS  
 K/S2  
 r.64  
 SMIN=0  
 -S=1.2,4,8,16  
 PW 1.1,1

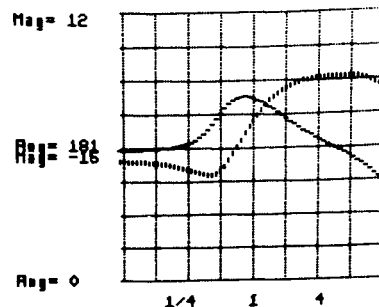


Mag 6 db/grid  
 Ang 45 deg/grid  
 W from to 16 rad/sec  
 tape block 4645 set 3  
 points 50 to 250

d

Bode Plot

8364-3  
 XE-XS  
 ONE AXIS  
 INPUT r.64  
 K/S2  
 SMIN=0  
 -S=1.2,4,8,16  
 PW 1.1,1

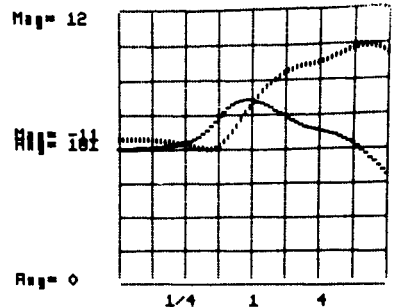


Mag 6 db/grid  
 Ang 45 deg/grid  
 W from to 16 rad/sec  
 tape block 1507 set 4  
 points 50 to 250

b

Bode Plot

91864-8a  
 XE-XS  
 ONE AXIS  
 K/S2  
 r.64  
 SMIN=0  
 -S=1.2,4,8,16  
 PW 1.1,1

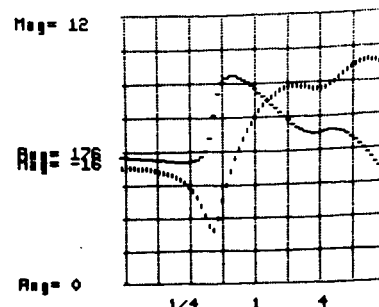


Mag 6 db/grid  
 Ang 45 deg/grid  
 W from to 16 rad/sec  
 tape block 4645 set 4  
 points 50 to 250

e

Bode Plot

8364-3  
 XE-XS  
 ONE AXIS  
 INPUT r.64  
 K/S2  
 SMIN=0  
 -S=1.2,4,8,16  
 PW 1.1,1

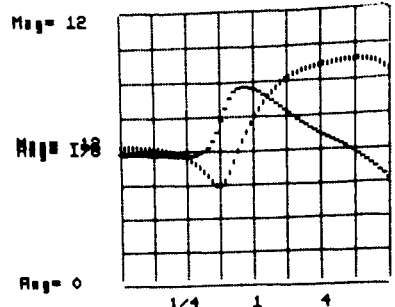


Mag 6 db/grid  
 Ang 45 deg/grid  
 W from to 16 rad/sec  
 tape block 1507 set 5  
 points 50 to 250

c

Bode Plot

91864-8a  
 XE-XS  
 ONE AXIS  
 K/S2  
 r.64  
 SMIN=0  
 -S=1.2,4,8,16  
 PW 1.1,1

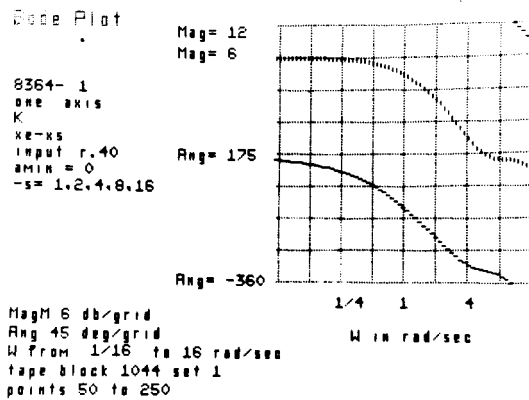


Mag 6 db/grid  
 Ang 45 deg/grid  
 W from to 16 rad/sec  
 tape block 4645 set 5  
 points 50 to 250

f

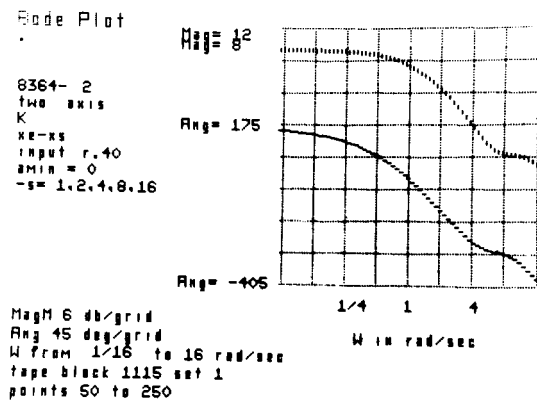
# FIG. 10 HUMAN OPERATOR DESCRIBING FUNCTIONS. CHANGES WITH DYNAMICS

## Single-axis Tracking



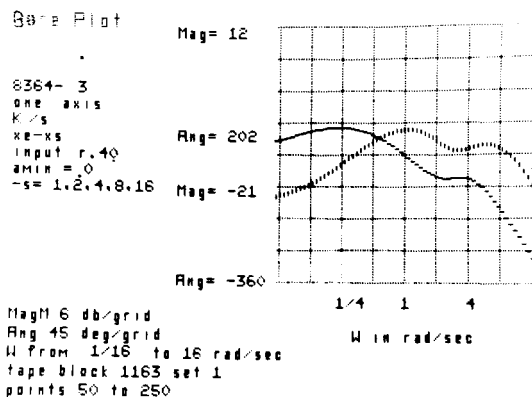
a

## Two-axis Tracking

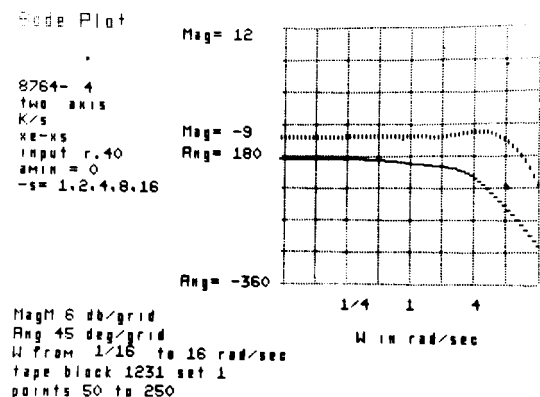


b

$$C_{xx} = C_{yy} = K$$

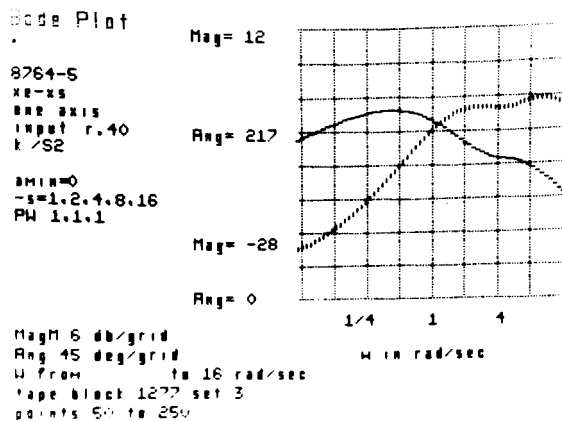


c

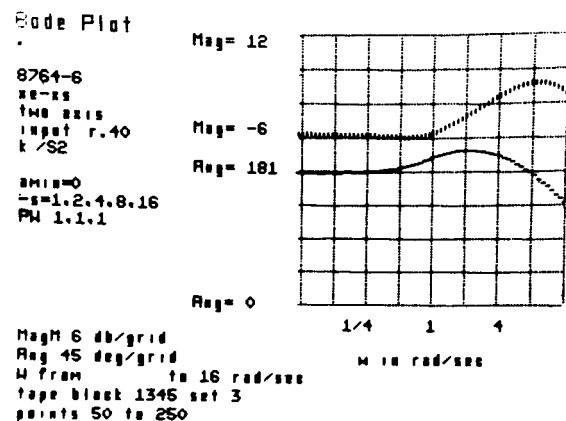


d

$$C_{xx} = C_{yy} = K/s$$



e



f

$$C_{xx} = C_{yy} = K/s^2$$

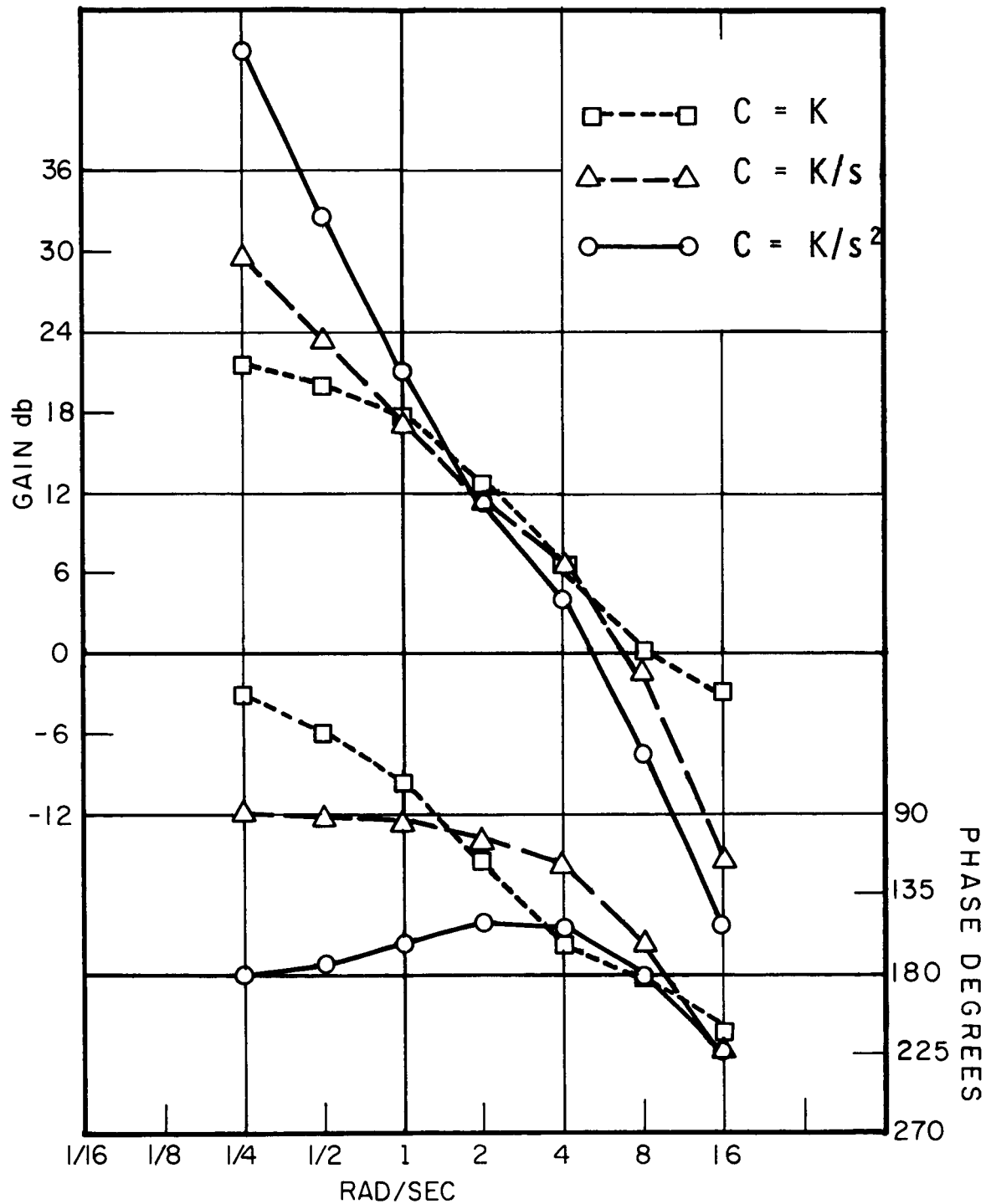


FIG. 11 OPEN LOOP DESCRIBING FUNCTIONS  
CHANGES WITH DYNAMICS  
 $w_i = 2.5 \text{ RAD/SEC}$

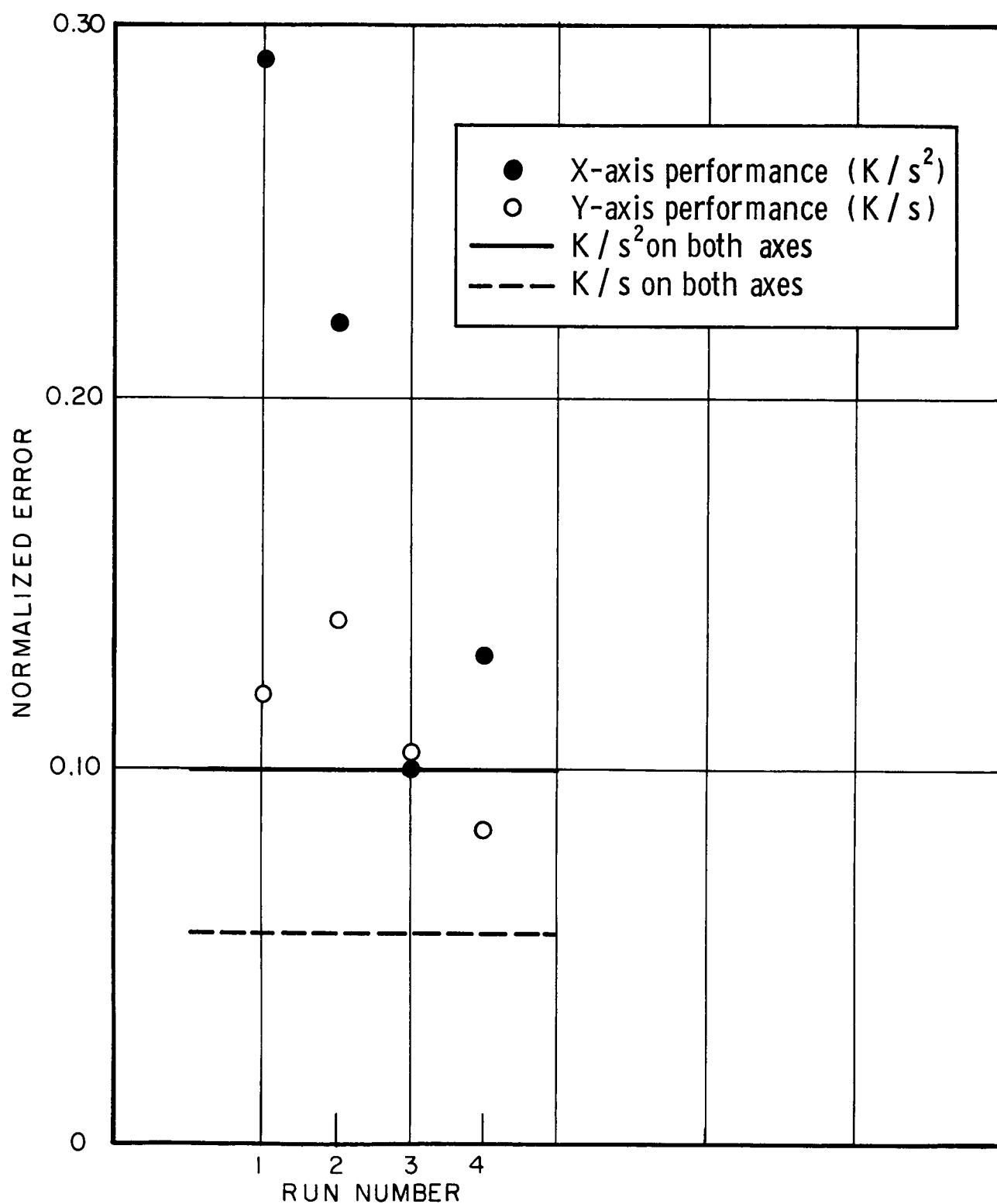


FIG. 12 PERFORMANCE WITH DIFFERENT DYNAMICS  
ON EACH AXIS  
VELOCITY CONTROL ON Y AXIS  
ACCLERATION CONTROL ON X AXIS  
 $w_i = 2.5 \text{ RAD/SEC}$

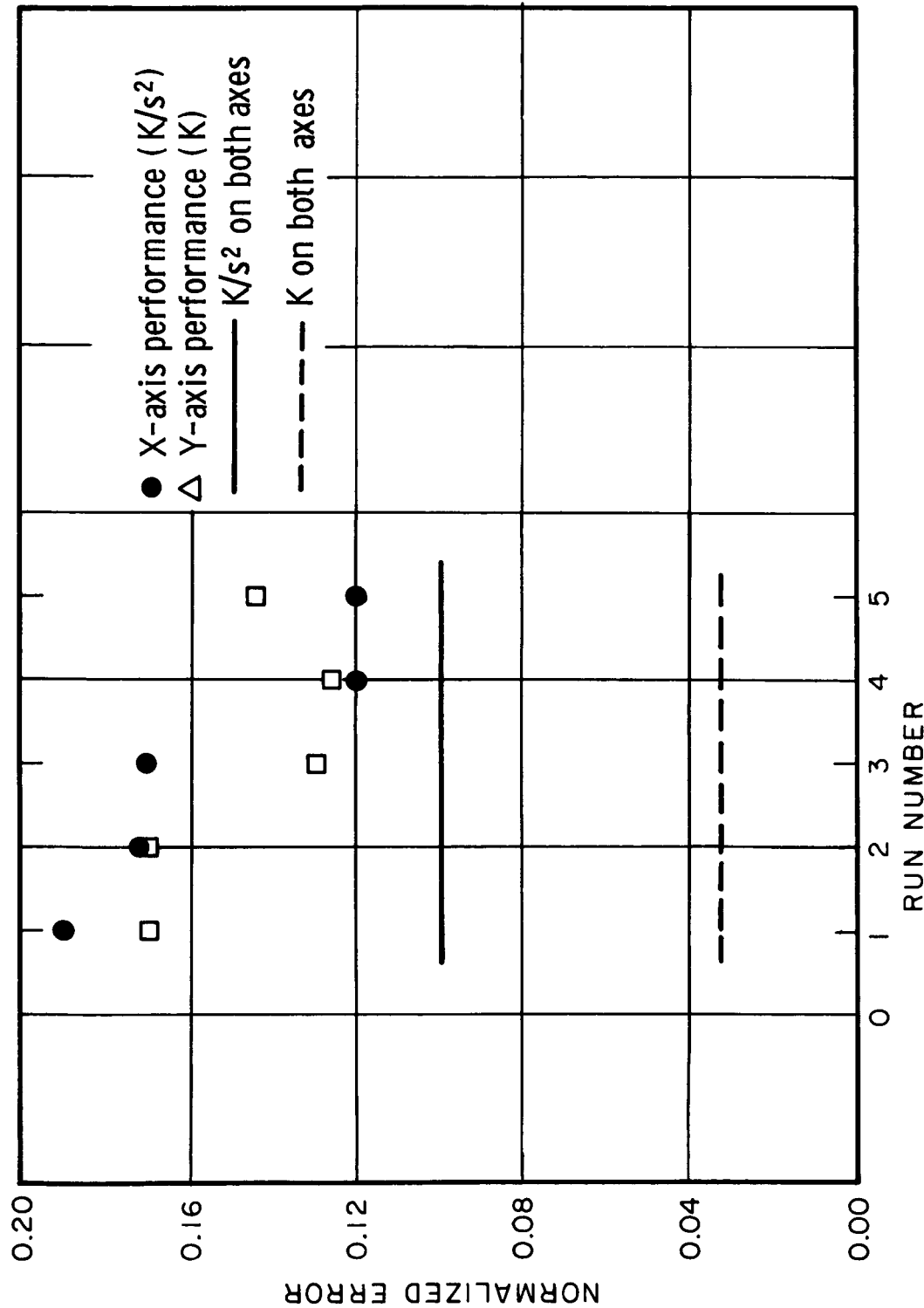


FIG. 13 PERFORMANCE WITH. DIFFERENT DYNAMICS ON EACH AXIS  
PROPORTIONAL CONTROL ON Y AXIS  
ACCELERATION CONTROL ON X AXIS  
 $w_i = 2.5 \text{ RAD/SEC}$

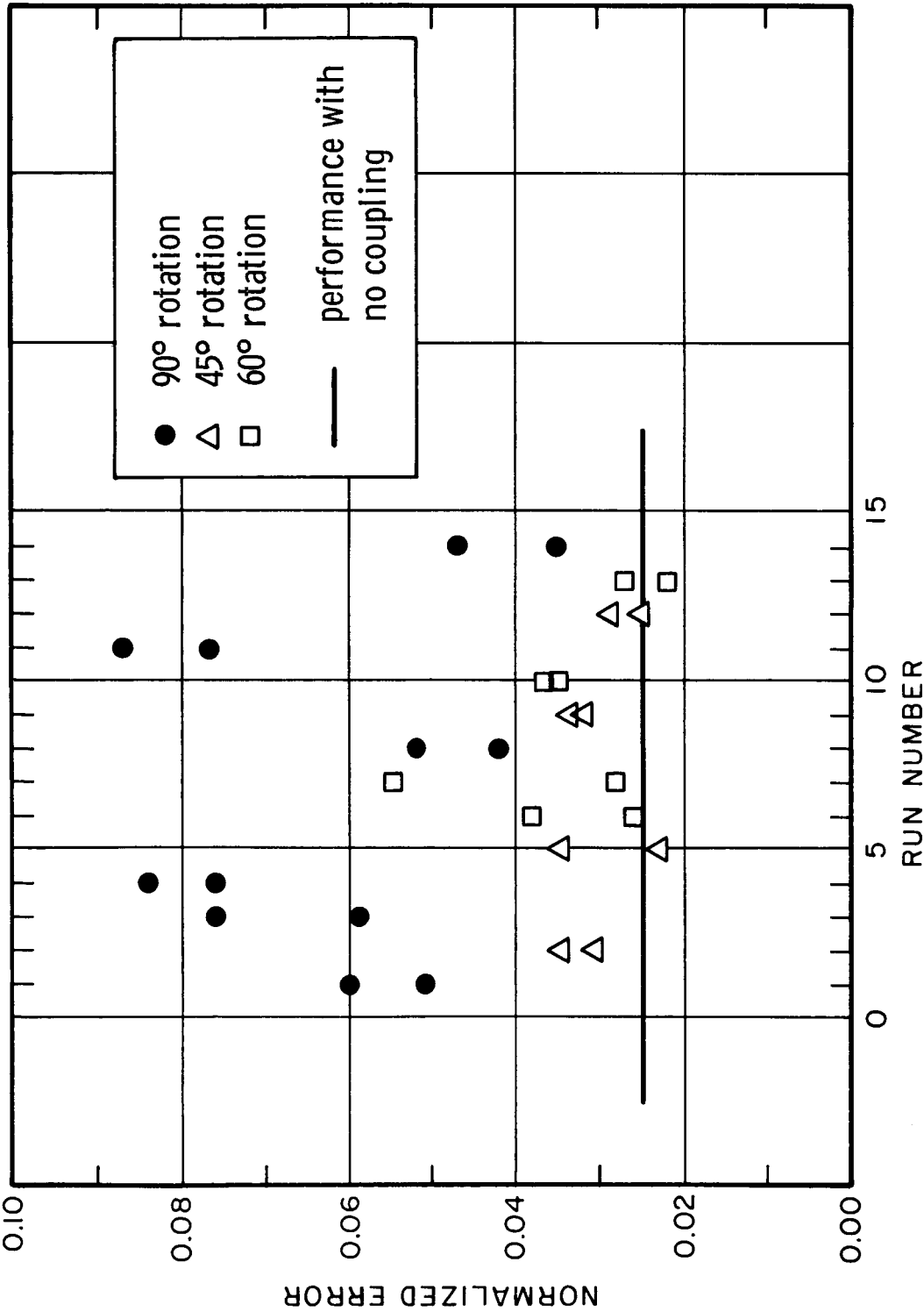


FIG. 14 INPUT COUPLING

$C_{xx} = C_{yy} = K/s^2$

$w_i = 1.5 \text{ RAD/SEC}$



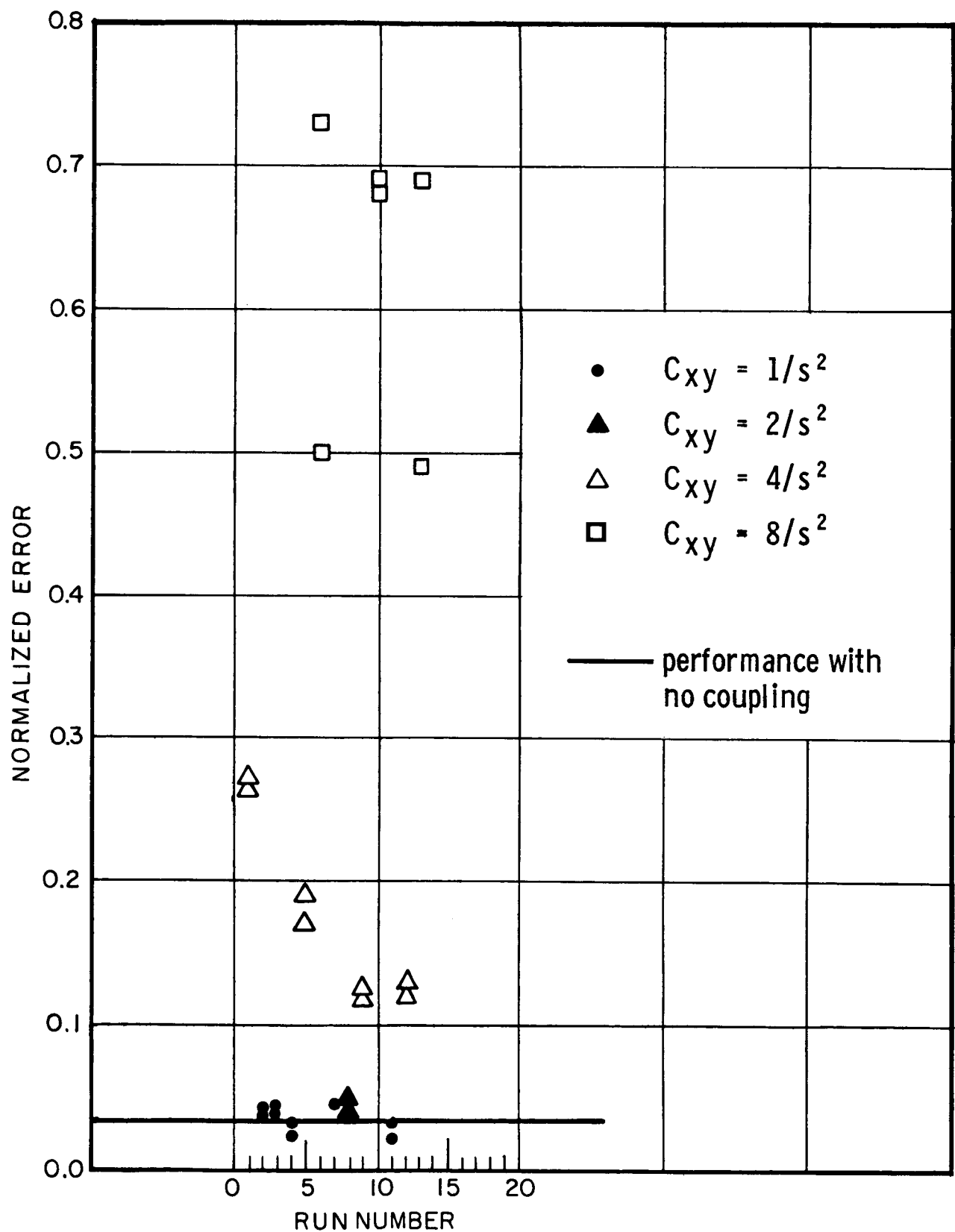


FIG. 15 OUTPUT COUPLING  
 $C_{xx} = C_{yy} = K/s^2$

$w_i = 1.5 \text{ RAD/SEC}$